Interfacial fluid flow for systems with anisotropic roughness

B.N.J. $Persson^{1,2,a}$

¹ PGI-1, FZ Jülich, Jülich, Germany

Received 5 March 2020 and Received in final form 15 April 2020

Published online: 25 May 2020

© The Author(s) 2020. This article is published with open access at Springerlink.com

Abstract. I discuss fluid flow at the interface between solids with anisotropic roughness. I show that the Bruggeman effective medium theory and the critical junction theory give nearly the same results for the fluid flow conductivity. This shows that, in most cases, the surface roughness observed at high magnification is irrelevant for fluid flow problems such as the leakage of static seals, and fluid squeeze-out. The effective medium theory predicts that the fluid flow conductivity vanishes at the relative contact area $A/A_0 = 0.5$ independent of the anisotropy. However, the effective medium theory does not solve the elastic contact mechanics problem but is based on a purely geometric argument. Thus, for anisotropic roughness the contact area may percolate at different values of A/A_0 depending on the direction. We discuss how this may be taken into account in the effective medium and critical junction theories.

1 Introduction

Fluid flow at the interface between elastic solids is a complicated topic, in general involving elastic deformations, complex fluid rheology and interfacial fluid slip [1]. In particular, the influence of the surface roughness on the fluid flow dynamics is a highly complex topic. However, if there is a separation of length scales the problem can be simplified: if R denotes the (smallest) macroscopic radius of curvature of the (undeformed) surfaces in the nominal contact region, e.g., the radius of a ball, and if $R \gg \lambda_0$, where λ_0 is the longest (relevant) surface roughness component, then it is possible to eliminate (integrate out) the surface roughness and obtain effective fluid flow equations involving solid bodies with smooth surfaces (no roughness). The effective fluid flow equations depend on quantities determined by the surface roughness, usually denoted fluid flow and friction factors (there are two fluid flow factors and three friction factors). These factors depend on the average surface separation \bar{u} , which will vary throughout the nominal contact region; \bar{u} is the local interfacial surface separation u(x,y) averaged over the surface roughness [2, 3]. In several publications it has been shown how to calculate the fluid flow factors, which enter in the (modified) Reynolds equation, and the friction factors, which enter in the expression for the shear stress acting on the solids [1, 4-10].

Here we consider the simplest fluid flow problems, which include the leakage of static seals [11, 12] and the

$$\bar{\mathbf{J}} = -\sigma_{\text{eff}} \nabla \bar{p},$$

where $\bar{p} = \langle p(x,y) \rangle$ is the fluid pressure and $\bar{\mathbf{J}} = \langle \mathbf{J}(x,y) \rangle$ the two-dimensional (2D) fluid flow current, both averaged over the surface roughness (ensemble averaging). The flow conductivity σ_{eff} is a 2 × 2 matrix (tensor).

As an example, consider a seal consisting of a rubber block with square cross section $L \times L$, with surface roughness on length scales much smaller than L, squeezed against a flat surface (see fig. 1). Assume that a high pressure fluid occurs for x < 0 and a low pressure fluid for x > L (pressure difference $\Delta P = P_{\rm a} - P_{\rm b} > 0$). In this case for the chosen coordinate system $\sigma_{\rm eff}$ is a diagonal matrix:

$$\sigma_{\text{eff}} = \begin{pmatrix} \sigma_x & 0 \\ 0 & \sigma_y \end{pmatrix}.$$

The pressure gradient $\nabla \bar{p}$ is along the x-axis and $\mathrm{d}\bar{p}/\mathrm{d}x = -\Delta P/L$. Thus, the fluid leakage rate (volume per unit time) becomes

$$\dot{Q} = LJ_x = L\sigma_x \Delta P/L = \sigma_x \Delta P.$$

From the fluid flow conductivity one can calculate the pressure flow factor

$$\phi_{\rm p} = 12 \eta \bar{u}^{-3} \sigma_{\rm eff}.$$

² MultiscaleConsulting, Wolfshovener str 2, 52428 Jülich, Germany

squeeze-out of fluids [13] between elastic solids. For these applications the roughness enter only via one function, namely the pressure flow factor $\phi_p(\bar{u})$ (in general a 2×2 tensor) or, equivalently, the (effective) fluid flow conductivity $\sigma_{\rm eff}$ defined by the equation

a e-mail: b.persson@fz-juelich.de

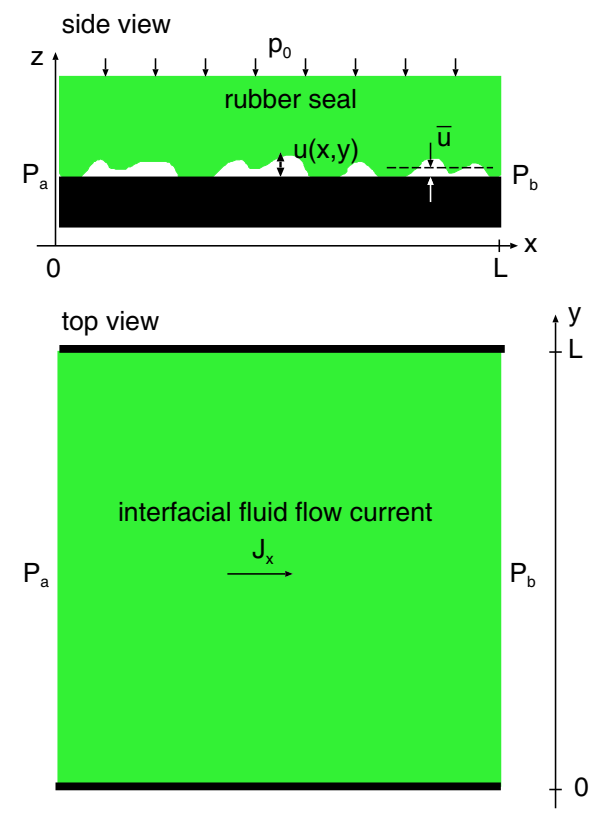


Fig. 1. A square block $L \times L$ rubber seal (green) with surface roughness squeezed with the uniform pressure p_0 against a flat rigid countersurface. A fluid pressure difference $\Delta P = P_a - P_b > 0$ occurs between the two sides x = 0 and x = L.

For two parallel surfaces without roughness one has the flow conductivity (Poiseuille flow):

$$\sigma_0 = \frac{u_0^3}{12\eta} \,,$$

where u_0 is the surface separation. For a system with surface roughness it is sometimes convenient to define a separation u_c , which depends on the average surface separation \bar{u} , so that

$$\sigma_{\rm eff} = \frac{u_{\rm c}^3}{12\eta} \,.$$

Thus the pressure flow factor

$$\phi_{\rm p} = \left(\frac{u_{\rm c}}{\bar{u}}\right)^3$$
.

When the average surface separation \bar{u} is much larger than the surface roughness amplitude, $u_{\rm c} \to \bar{u}$ and $\phi_{\rm p} \to 1$. Note also that when the area of real contact percolates no fluid flow at the interface is possible and $\sigma_{\rm eff}$ and $\phi_{\rm p}$ both vanish.

In this paper I discuss fluid flow at the interface between solids with anisotropic roughness. I show that in the Bruggeman effective medium theory the fluid flow conductivity for anisotropic roughness vanishes at the same relative contact area as for isotropic roughness. However, the effective medium theory does not involve solving the elastic contact mechanics problem, and the actual percolation threshold may depend on the surface roughness anisotropy as suggested by recent numerical contact mechanics studies [14–18]. I will discuss how this can be taken into account in the critical junction and the effective medium theories.

I also show that, unless the applied pressure is very small, the Bruggeman effective medium theory and the critical junction theory give nearly the same results for the fluid flow conductivity (and the fluid pressure flow factor). This shows that for applications which involve only the flow conductivity (or, equivalently, the pressure flow factor), such as the leakage of static seals and fluid squeeze-out, in most cases the (short wavelength) surface roughness observed at high magnification is irrelevant.

2 Qualitative discussion

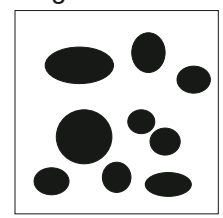
The theory of fluid flow discussed in this paper is based on the Bruggeman effective medium theory. This theory is for an infinite-sized system but real applications and computer simulations involve systems of finite sizes. Finite-size effects may in some cases be important, in particular for systems with strongly anisotropic roughness such as surfaces grinded in one direction, and for systems with small nominal contact area.

Consider the contact between two elastic solids with random surface roughness. One way to (mathematically) produce systems with anisotropic roughness is to start with a surface with isotropic roughness, say a square area of size $L \times L$, and stretch the surface in the x-direction be a factor $\gamma^{1/2}$ and contract it in the y-direction by a factor $\gamma^{-1/2}$, as indicated in fig. 2(b). This will map a circle on an ellipse (with the same surface area) where the ratio between the ellipse axis in the x- and y-directions is given by γ (Peklenik number [19]).

To get a square unit surface we extend the surface in the y-direction with similar rectangular units (but from other realizations, e.g., generated mathematically using different sets of random numbers) as in fig. 2(b), see fig. 2(c). If a surface region, with the same size $L \times L$ as the original surface, is cut-out of the surface in fig. 2(c), the contact area may percolate in the x-direction (see the dashed square in fig. 2(c)) even if the contact area did not percolate for the original surface. However, for the infinite system stretching the contact area obtained from isotropic roughness cannot change the percolation threshold. This is clear since a flow channel which is closed before stretching remain closed after stretching, and a flow channel which is open before stretching will remain open after stretching. Indeed, the Bruggeman theory predicts that the contact area percolates when $A = A_p$, where $A_p/A_0 = 0.5$ is independent of γ (see sect. 5).

Figure 2 illustrates the effect of stretching the *contact* area obtained from isotropic roughness. However, we are interested in stretching the *surface roughness* topography. Solving the elastic contact mechanics problem using the stretched surface roughness profile will result in a different

(a) original



stretched by factor 2 in x-direction and 1/2 in the y-direction



(c) stretched by factor 2 in x-direction, and 1/2 in the y-direction and extended in y-direction

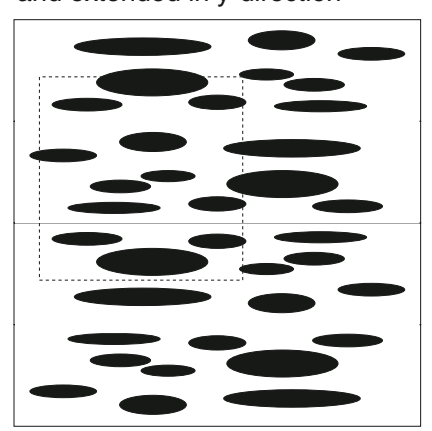


Fig. 2. (a) Asperity contact regions (black) for a system with random roughness with isotropic statistical properties, and (b) for a system obtained by stretching by a factor of 2 in the x-direction and 1/2 in the y-direction. This transformation conserves the area and results in anisotropic roughness with $\gamma=4$. (c) Adding 4 different realizations of the stretched roughness gives a square unit with anisotropic roughness. For a system of finite size, if the system size is fixed (compare (a) with the dashed square in (c)) the contact area percolation threshold depends on the stretching factor γ , but for an infinite system the percolation threshold does not depend on γ .

contact area morphology than just stretching the contact area obtained for the isotropic roughness. The Bruggeman effective medium theory for anisotropic systems is based on stretching the contact area (as in fig. 2), and may therefore give wrong predictions for the γ -dependence of A/A_0 at percolation threshold.

In ref. [14] I presented an approximate formula for the fluid flow conductivity which interpolates between the Bruggeman effective medium theory result for isotropic roughness, and the known limit for the fluid flow conductivity for the case of strongly anisotropic roughness. The expression for the flow conductivity σ_x proposed in ref. [14] is

$$\frac{1}{\sigma_x} = \left\langle \frac{1+\gamma}{\sigma + \gamma \sigma_x} \right\rangle,\tag{1}$$

where $\sigma = u^3/(12\eta)$, where η is the fluid viscosity and $u = u(\mathbf{x})$ the interfacial separation at the point $\mathbf{x} = (x, y)$. The $\langle \ldots \rangle$ stands for ensemble averaging, or averaging over the probability distribution P(u) of interfacial separations. For $\gamma = 1$ this equation reduces to the standard Bruggeman equation for isotropic roughness, while for $\gamma \to 0$ it gives $\sigma_x = \langle \sigma^{-1} \rangle^{-1}$ and for $\gamma \to \infty$ it gives $\sigma_x = \langle \sigma \rangle$. Both these limits are exact results as is easy to show directly from the Reynolds equation for thin-film fluid flow.

The flow conductivity in the y-direction is obtained from (1) by replacing γ with $1/\gamma$:

$$\frac{1}{\sigma_y} = \left\langle \frac{1 + (1/\gamma)}{\sigma + (1/\gamma)\sigma_y} \right\rangle. \tag{2}$$

We can write the probability distribution of interfacial separation as [20, 21]

$$P(u) = \frac{A}{A_0}\delta(u) + P_{\rm c}(u),\tag{3}$$

where $P_{c}(u)$ is the (continuous) part of the distribution where u > 0. Thus we get

$$\frac{1}{\sigma_x} = \frac{1+\gamma}{\sigma_x \gamma} \frac{A}{A_0} + \left\langle \frac{1+\gamma}{\sigma + \gamma \sigma_x} \right\rangle_{c}.$$
 (4)

When the contact area percolates, $A = A_p$, no fluid flow is possible from one side to the other side of the studied unit, so that $\sigma_x \to 0$. When $\sigma_x \to 0$ using (4) gives

$$1 = \frac{1 + \gamma}{\gamma} \frac{A_{\rm p}}{A_0} \,,$$

or $A_{\rm p}/A_0 = \gamma/(1+\gamma)$. However, a more accurate study (see sects. 4 and 5) shows that the effective medium predicts that the relative contact area A/A_0 at the percolation threshold does not depend on γ .

Computer simulations of contact mechanics are always for finite-sized systems. In this case it has been observed [14–18] that when $\gamma > 1$ the contact area percolates for a smaller relative contact area $A_{\rm p}/A_0$ than when $\gamma = 1$. Similarly, for $\gamma < 1$ the contact area percolates for a larger $A_{\rm p}/A_0$ than when $\gamma = 1$, and in one study the results was rather accurately described by the formula $A_{\rm p}/A_0 = \gamma/(1+\gamma)$. These results are intuitively clear, but the simulation results depend on the system size, and this is hence non-universal. However, a recent study using different system sizes indicates that the A/A_0 at the percolation threshold depends on γ even as the system size approaches infinite.

The Bruggeman effective medium theory gives flow conductivities of the form (1) and (2), but with γ replaced by $\gamma^* = \gamma (\sigma_y/\sigma_x)^{1/2}$ (see sect. 4). For this case the percolation threshold occurs when $A/A_0 = 0.5$ independent of γ (see sect. 5).

3 Tripp number

The most important property characterizing a rough surface is the surface roughness power spectrum $C(\mathbf{q})$. If $z = h(\mathbf{x})$ is the height coordinate at the point $\mathbf{x} = (x, y)$ then the two-dimensional (2D) power spectrum $C(\mathbf{q}) = C(q_x, q_y)$ is given by

$$C(\mathbf{q}) = \frac{1}{(2\pi)^2} \int d^2x \langle h(\mathbf{x})h(\mathbf{0})\rangle e^{i\mathbf{q}\cdot\mathbf{x}}, \qquad (5)$$

where $\langle \ldots \rangle$ stands for ensemble averaging. For a surface with isotropic statistical properties, $C(\mathbf{q})$ depends only on the magnitude $q=|\mathbf{q}|$ of the 2D wave vector \mathbf{q} . For surfaces with anisotropic statistical properties the Tripp number [9] $\gamma(q)$ is very important as it determines the influence of the surface roughness anisotropy on interfacial fluid flow [9,22]. The Tripp number depends on the length scale considered, *i.e.*, it is a function of the wavenumber q, and is defined as follows [22]. We introduce polar coordinates $\mathbf{q} = q(\cos\phi, \sin\phi)$ and define the matrix

$$D(q) = \frac{\int_0^{2\pi} d\phi \, C(\mathbf{q}) \mathbf{q} \mathbf{q}/q^2}{\int_0^{2\pi} d\phi \, C(\mathbf{q})}.$$
 (6)

Note that D(q) is a symmetric matrix and can be diagonalized by an orthogonal transformation. We denote the diagonal elements by $1/(1+\gamma)$ and $\gamma/(1+\gamma)$ where $\gamma=\gamma(q)$ is the Tripp number, which depends on the wavenumber q. If $C(\mathbf{q})$ only depends on the magnitude of the wavevector then $D_{ij}(q)=\delta_{ij}/2$, so that $\gamma=1$ for roughness with isotropic statistical properties.

One can also define the average Tripp number using

$$D = \frac{\int d^2 q \, C(\mathbf{q}) \mathbf{q} \mathbf{q}/q^2}{\int d^2 q \, C(\mathbf{q})}.$$
 (7)

Let us study

$$I = \int \mathrm{d}^2 q \, C(\mathbf{q}) \frac{\mathbf{q}\mathbf{q}}{a^2}$$

for a particular case. Assume that f(x,y) = f(r) only depends on the magnitude of the coordinate \mathbf{x} and consider the function $f(x/a_x,y/a_y)$. If f(r)=0 is a circle then $f(x/a_x,y/a_y)=0$ is an ellipse. In wavevector space we get the function $g(q_xa_x,q_ya_y)$. Assume that $C(\mathbf{q})=g(q_xa_x,q_ya_y)$ with $g(q_x,q_y)=g(q)$. Writing $q_x'=q_xa_x$, $q_y'=q_ya_y$ we get

$$I = \frac{1}{a_x a_y} \int d^2 q' \, g(q') \frac{1}{(q'_x/a_x)^2 + (q'_y/a_y)^2} \times \begin{pmatrix} (q'_x/a_x)^2 & q'_x q'_y/(a_x a_y) \\ q'_x q'_y/(a_x a_y) & (q'_y/a_y)^2 \end{pmatrix}.$$

In polar coordinates

$$q'_x = q'\cos\phi, \qquad q'_y = q'\sin\phi$$

we get

$$I = \frac{1}{a_x a_y} \int d^2 q' \, g(q') \frac{1}{a_x^{-2} \cos^2 \phi + a_y^{-2} \sin^2 \phi} \times \begin{pmatrix} a_x^{-2} \cos^2 \phi & (a_x a_y)^{-1} \cos \phi \sin \phi \\ (a_x a_y)^{-1} \cos \phi \sin \phi & a_y^{-2} \sin^2 \phi \end{pmatrix}$$

or

$$I = \frac{1}{a_x a_y} \int d^2 q' \, g(q') \frac{1}{\cos^2 \phi + \gamma^2 \sin^2 \phi} \times \begin{pmatrix} \cos^2 \phi & 0\\ 0 & \gamma^2 \sin^2 \phi \end{pmatrix}. \tag{8}$$

Let us denote $a_x/a_y = \gamma$ which we refer to as the Tripp number. Since g(q') only depends on the magnitude of \mathbf{q}' we can write (8) as

$$\begin{split} I &= \frac{1}{a_x a_y} \int \mathrm{d}^2 q' \, g(q') \frac{1}{2\pi} \int \mathrm{d}\phi \frac{1}{\cos^2 \phi + \gamma^2 \sin^2 \phi} \\ &\quad \times \begin{pmatrix} \cos^2 \phi & 0 \\ 0 & \gamma^2 \sin^2 \phi \end{pmatrix}. \end{split}$$

Finally using that

$$\frac{1}{a_x a_y} \int d^2 q' g(q') = \int d^2 q g(q_x a_x, q_y a_y) = \int d^2 q C(\mathbf{q}),$$

we get

$$D = \frac{1}{2\pi} \int d\phi \frac{1}{\cos^2 \phi + \gamma^2 \sin^2 \phi} \begin{pmatrix} \cos^2 \phi & 0 \\ 0 & \gamma^2 \sin^2 \phi \end{pmatrix}.$$

The integral over ϕ is easy to perform (see appendix A) giving

$$D = \frac{1}{1+\gamma} \begin{pmatrix} 1 & 0 \\ 0 & \gamma \end{pmatrix}. \tag{9}$$

Note that the matrix D is a symmetric matrix which can be diagonalized. Since $\operatorname{Tr} D=1$, in the coordinate system where D is diagonal there is only one number (here denoted γ) characterizing D. Thus we can always write D on the form (9) in the coordinate system where it is diagonal even if $C(q_x,q_y)$ is not of the form assumed above. In general, it is always possible to generate surfaces with anisotropic roughness which has an angular averaged power spectrum which is self-affine fractal, and with asymmetry characterized by the Tripp number γ .

4 Bruggeman effective medium theory for fluid flow

Effective medium theories are simple, but very useful and often accurate methods to describe some properties of inhomogeneous materials. The effective medium approach assumes that the material in randomly disordered at length scales much shorter than the length scale of

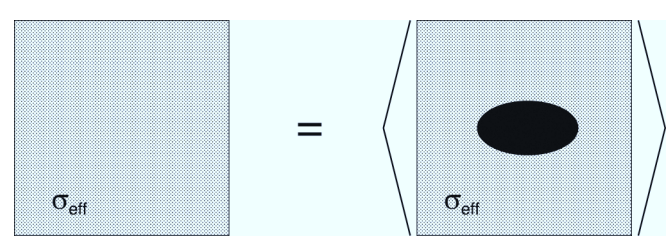


Fig. 3. In the effective medium approach a system with anisotropic roughness is replaced by an effective system with the (constant) flow conductivity $\sigma_{\rm eff}$. The effective flow conductivity is determined as follows: An elliptic region with the constant surface separation u is embedded in the effective medium. The flow current $\mathbf{J}_u(x,y)$ for this system depends on the surface separation u in the elliptic region. The effective conductivity is determined by the condition that \mathbf{J}_u averaged over the probability distribution of surface separations P(u) is equal to the flow current obtained using the effective medium everywhere.

interest. Typical applications of effective medium theories are the optical properties of inhomogeneous materials, and the electric or fluid transport in inhomogeneous materials. There are several different (but related) effective medium theories, e.g. the coherent potential approximation or the Bruggeman effective medium approximation [15–17,23–27]. In earlier publications we have shown how the leakage of seals can be accurately described using the Bruggeman effective medium theory for systems with random but isotropic surface roughness [12].

The fluid flow current

$$\mathbf{J} = -\sigma \nabla p,\tag{10}$$

where

$$\sigma = \frac{u^3}{12\eta} \,, \tag{11}$$

where $u(\mathbf{x})$ is the interfacial separation at the point \mathbf{x} and η the fluid viscosity. Conservation of mass

$$\nabla \cdot \mathbf{J} = 0. \tag{12}$$

We will replace the inhomogeneous system with a homogeneous system with the average interfacial separation $\bar{u}(\mathbf{x})$ which can be treated locally as a constant. The average flow current

$$\bar{\mathbf{J}} = -\sigma_{\text{eff}} \nabla \bar{p}. \tag{13}$$

The flow conductivity $\sigma_{\rm eff}$ in the Bruggeman effective medium approach is determined as indicated in fig. 3. That is, in the effective medium approach a system with anisotropic roughness is replaced by an effective system with the (constant) flow conductivity $\sigma_{\rm eff}$. The effective flow conductivity is determined as follows: An elliptic region with the constant surface separation u is embedded in the effective medium. The flow current $\mathbf{J}_u(x,y)$ for this system depends on the surface separation u in the elliptic region. The effective conductivity is determined by the condition that \mathbf{J}_u averaged over the probability distribution of surface separations P(u) is equal to the flow current obtained using the effective medium everywhere.

The treatment which follows is similar to those presented in refs. [24] and [25]. Let us write

$$\mathbf{J}_u = -\sigma \nabla p$$
, inside the elliptic region, (14)

$$\mathbf{J}_u = -\sigma_{\text{eff}} \nabla p$$
, outside the elliptic region. (15)

Thus if we define

$$\mathbf{J}_{u} = -\sigma_{\text{eff}} \nabla p + \mathbf{J}_{1},\tag{16}$$

then $\mathbf{J}_1 = \mathbf{0}$ outside the elliptic region. Using (12) we get

$$\nabla \cdot \sigma_{\text{eff}} \nabla p = \nabla \cdot \mathbf{J}_1 = \int d^2 x' \delta(\mathbf{x} - \mathbf{x}') \nabla \cdot \mathbf{J}_1(\mathbf{x}'). \quad (17)$$

If we define

$$\nabla \cdot \sigma_{\text{eff}} \nabla G(\mathbf{x} - \mathbf{x}') = \delta(\mathbf{x} - \mathbf{x}'), \tag{18}$$

we can write

$$\nabla \cdot \left[\sigma_{\text{eff}} \left(\nabla p - \int d^2 x' \nabla G(\mathbf{x} - \mathbf{x}') \nabla' \cdot \mathbf{J}_1(\mathbf{x}') \right) \right] = 0.$$

This equation is satisfied by

$$\nabla p - \int d^2 x' \nabla G(\mathbf{x} - \mathbf{x}') \nabla' \cdot \mathbf{J}_1(\mathbf{x}') = \nabla p^o,$$

where ∇p^o is a constant vector. Thus

$$\nabla p = \nabla p^{o} + \int d^{2}x' \nabla \nabla G(\mathbf{x} - \mathbf{x}') \cdot \mathbf{J}_{1}(\mathbf{x}'), \qquad (19)$$

where we have performed a partial integration and used that $J_1(\mathbf{x})$ vanishes outside the elliptic region.

The problem above involves equations very similar to those in electrostatics (see appendix B). From electrostatics we know that if an elliptic (homogeneous) body is embedded in a (homogeneous) dielectric media, in an applied electric field the electric polarization in the inclusion is uniform. In the present case this implies that \mathbf{J}_1 is constant in the elliptic region where the interfacial separation equals u (a constant). Since \mathbf{J}_1 vanishes outside the elliptic region, if we define $f(\mathbf{x}) = 1$ inside the elliptic region and $f(\mathbf{x}) = 0$ outside, we can write (19) as

$$\nabla p = \nabla p^o + Q \cdot \mathbf{J}_1, \tag{20}$$

where the matrix

$$Q = \int d^2x f(\mathbf{x}) \nabla \nabla G(\mathbf{x}), \qquad (21)$$

where the integral is over the whole xy-plane. Since $\mathbf{J}_u = -\sigma \nabla p$ inside the elliptic region (see (14)) from (16) we get

$$\mathbf{J}_1 = (\sigma_{\text{eff}} - \sigma) \nabla p. \tag{22}$$

Substituting this in (20) gives

$$\nabla p = \nabla p^o + Q \cdot (\sigma_{\text{eff}} - \sigma) \nabla p.$$

or

$$[1 - Q \cdot (\sigma_{\text{eff}} - \sigma)] \nabla p = \nabla p^{o},$$

or

$$\nabla p = \left[1 - Q \cdot (\sigma_{\text{eff}} - \sigma)\right]^{-1} \nabla p^{o}. \tag{23}$$

Using (22) and (23) we get

$$\mathbf{J}_1 = (\sigma_{\text{eff}} - \sigma) \nabla p = (\sigma_{\text{eff}} - \sigma) \left[1 - Q \cdot (\sigma_{\text{eff}} - \sigma) \right]^{-1} \nabla p^o.$$

We demand that the average of J_1 vanishes which gives

$$\langle \mathbf{J}_1 \rangle = \langle (\sigma_{\text{eff}} - \sigma) \left[1 - Q \cdot (\sigma_{\text{eff}} - \sigma) \right]^{-1} \rangle \nabla p^o = 0.$$

Since ∇p^o is an arbitrary constant vector we get

$$\langle (\sigma_{\text{eff}} - \sigma) \left[1 - Q \cdot (\sigma_{\text{eff}} - \sigma) \right]^{-1} \rangle = 0.$$
 (24)

Since Q is a diagonal matrix (see below) with components Q_{11} and Q_{22} , the matrix $M = [1 - Q \cdot (\sigma_{\text{eff}} - \sigma)]$ is also diagonal with the elements

$$M_{11} = 1 - Q_{11}(\sigma_x - \sigma)$$

and

$$M_{22} = 1 - Q_{22}(\sigma_y - \sigma).$$

Thus, we get from (24):

$$\left\langle \frac{\sigma_x - \sigma}{1 - Q_{11}(\sigma_x - \sigma)} \right\rangle = 0, \tag{25}$$

$$\left\langle \frac{\sigma_y - \sigma}{1 - Q_{22}(\sigma_y - \sigma)} \right\rangle = 0. \tag{26}$$

The Fourier transform of (18) gives

$$-\mathbf{q} \cdot \sigma_{\text{eff}} \mathbf{q} G(\mathbf{q}) = \frac{1}{(2\pi)^2} \,,$$

or

$$G(\mathbf{q}) = -\frac{1}{(2\pi)^2} \frac{1}{\sigma_x a_x^2 + \sigma_y a_y^2}$$
 (27)

and (21) gives

$$Q = \int d^2x \int d^2q \, d^2q' \, f(\mathbf{q}')(-\mathbf{q}\mathbf{q})G(\mathbf{q})e^{i(\mathbf{q}+\mathbf{q}')\cdot\mathbf{x}}$$
$$= (2\pi)^2 \int d^2q \, f(\mathbf{q})(-\mathbf{q}\mathbf{q})G(\mathbf{q}). \tag{28}$$

Using (27) and (28) and $q'_x = q_x a_x$, $q'_y = q_y a_y$ and using that $f(\mathbf{q}) = f(q')$ we get

$$\begin{split} Q &= \frac{1}{a_x a_y} \int \mathrm{d}^2 q' \, f(q') \frac{1}{\sigma_x (q_x'/a_x)^2 + \sigma_y (q_y'/a_y)^2} \\ &\times \begin{pmatrix} (q_x'/a_x)^2 & q_x' q_y'/(a_x a_y) \\ q_x' q_y'/(a_x a_y) & (q_y'/a_y)^2 \end{pmatrix}, \end{split}$$

or

$$\begin{split} Q &= \frac{1}{a_x a_y} \int \mathrm{d}^2 q' \, f(q') \frac{1}{2\pi} \int \mathrm{d}\phi \\ &\times \frac{1}{\sigma_x a_x^{-2} \cos^2 \phi + \sigma_y a_y^{-2} \sin^2 \phi} \\ &\times \begin{pmatrix} a_x^{-2} \cos^2 \phi & (a_x a_y)^{-1} \cos \phi \sin \phi \\ (a_x a_y)^{-1} \cos \phi \sin \phi & a_y^{-2} \sin^2 \phi \end{pmatrix}. \end{split}$$

Using that

$$\frac{1}{a_x a_y} \int d^2 q' f(q') = \int d^2 q f(\mathbf{q}) = f(\mathbf{x} = \mathbf{0}) = 1,$$

we get

$$\begin{split} Q &= \frac{1}{2\pi} \int \mathrm{d}\phi \, \frac{1}{\sigma_x a_x^{-2} \cos^2\phi + \sigma_y a_y^{-2} \sin^2\phi} \\ &\quad \times \left(\begin{array}{c} a_x^{-2} \cos^2\phi & (a_x a_y)^{-1} \cos\phi\sin\phi \\ (a_x a_y)^{-1} \cos\phi\sin\phi & a_y^{-2} \sin^2\phi \end{array} \right) \\ &= \frac{1}{2\pi\sigma_x} \int \mathrm{d}\phi \, \frac{1}{\cos^2\phi + \gamma^2(\sigma_y/\sigma_x)\sin^2\phi} \\ &\quad \times \left(\begin{array}{c} \cos^2\phi & 0 \\ 0 & \gamma^2 \sin^2\phi \end{array} \right). \end{split}$$

Using (A.1) and (A.2) this gives

$$Q_{11} = \frac{1}{\sigma_x} \frac{1}{1 + \gamma (\sigma_y / \sigma_x)^{1/2}}, \qquad (29)$$

$$Q_{22} = \frac{1}{\sigma_y} \frac{\gamma(\sigma_y/\sigma_x)^{1/2}}{1 + \gamma(\sigma_y/\sigma_x)^{1/2}}.$$
 (30)

Substituting (29) in (25) and (30) in (26) gives

$$\frac{1}{\sigma_x} = \left\langle \frac{1 + \gamma^*}{\sigma + \gamma^* \sigma_x} \right\rangle,\tag{31}$$

$$\frac{1}{\sigma_y} = \left\langle \frac{1 + (1/\gamma^*)}{\sigma + (1/\gamma^*)\sigma_y} \right\rangle,\tag{32}$$

where $\gamma^* = \gamma (\sigma_y/\sigma_x)^{1/2}$.

5 Limiting cases

Consider first the case when $\gamma^* \to \infty$. In this case from (31) we get $\sigma_x = \langle \sigma \rangle$ and from (32) $\sigma_y = \langle \sigma^{-1} \rangle^{-1}$. Note that

$$\gamma^* = \gamma \left(\frac{\sigma_y}{\sigma_x}\right)^{1/2} = \frac{\gamma}{(\langle \sigma \rangle \langle \sigma^{-1} \rangle)^{1/2}}.$$

Thus if $\gamma \to \infty$ it follows that $\gamma^* \to \infty$.

Note that when $\gamma^* \to \infty$, if the area of real contact A>0 we get $\langle u^{-1}\rangle^{-1}=0$, so that $\sigma_y=0$ and no fluid can flow in the y-direction. This result is clear from a physical point of view since strips of contact will extend between the two edges of the system in the x-direction as indicated in fig. 4 and no fluid flow is possible in the y-direction. The results for σ_x and σ_y when $\gamma \to \infty$ (or $\gamma \to 0$) are well known and can be easily obtained directly from the Reynold thin-film fluid flow equation with u(x,y) only depending on y (or x).

Next, let us consider the case when we increase the nominal contact pressure so we approach the limit when the contact area percolates. When the contact area percolates no fluid flow is possible from one side to the other

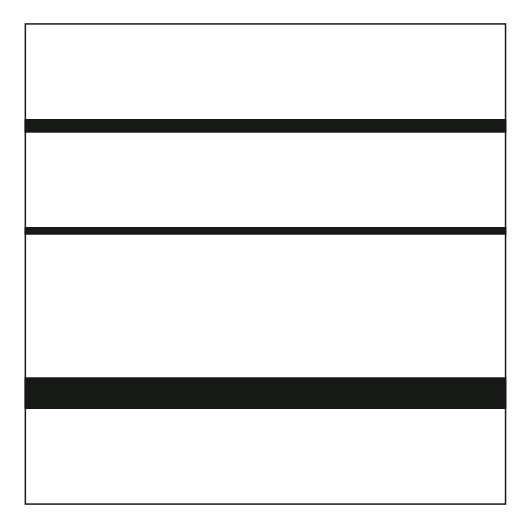


Fig. 4. Example of area of real contact (black) as $\gamma \to \infty$.

side of the studied unit, so that $\sigma_x \to 0$. We can write the probability distribution of interfacial separation as [20,21]

$$P(u) = \frac{A}{A_0}\delta(u) + P_{c}(u),$$

where $P_{\rm c}(u)$ is the part of the distribution where u > 0. Thus we get

$$\frac{1}{\sigma_x} = \frac{1 + \gamma^*}{\sigma_x \gamma^*} \frac{A}{A_0} + \left\langle \frac{1 + \gamma^*}{\sigma + \gamma^* \sigma_x} \right\rangle_{\bullet}, \tag{33}$$

$$\frac{1}{\sigma_y} = \frac{1 + \gamma^*}{\sigma_y} \frac{A}{A_0} + \left\langle \frac{1 + (1/\gamma^*)}{\sigma + (1/\gamma^*)\sigma_y} \right\rangle_0, \tag{34}$$

where $\langle ... \rangle_c$ stands for averaging using $P_c(u)$ *i.e.*, over the non-contact surface area $A_0 - A$. From (33) as $\sigma_x \to 0$ we get

$$1 = \frac{1 + \gamma^*}{\gamma^*} \frac{A_{\rm p}}{A_0} \,. \tag{35}$$

We will now show that $\sigma_x \to 0$ imply $\sigma_y \to 0$ i.e. the contact area percolates in both the x- and y-directions at the same time. To prove this, assume that this is not the case so σ_y remains non-zero as $\sigma_x \to 0$. It then follows that $\gamma^* = \gamma (\sigma_y/\sigma_x)^{1/2} \to \infty$ as $\sigma_x \to 0$. In this case (35) gives $A/A_0 = 1$. This result is incorrect because we know that the contact area when $\gamma = 1$ percolates when $A/A_0 = 0.5$. Thus $\sigma_x \to 0$ implies $\sigma_y \to 0$ and from (34) we get

$$1 = (1 + \gamma^*) \frac{A_p}{A_0} \,. \tag{36}$$

Using (35) and (36) gives $\gamma^* = 1$ and $A_p/A_0 = 1/2$. Using $\gamma^* = \gamma (\sigma_y/\sigma_x)^{1/2}$ and $\gamma^* = 1$ we get $\sigma_x = \gamma^2 \sigma_y$, which holds as $\sigma_x \to 0$.

Finally, let us consider the case when the separation $u(\mathbf{x}) = \bar{u} + \delta u(\mathbf{x})$ where \bar{u} is the average separation and $\delta u/\bar{u} \ll 1$. This case was studied in appendix A in ref. [14] but where we now must replace γ with γ^* . However, since $\gamma^* = \gamma$ to zero order in δu the results derived in appendix A in ref. [14] are still valid and we conclude that

the effective medium theory results for σ_x and σ_y is exact to order δu^2 and that γ can be obtained from the matrix D involving only the surface roughness power spectrum.

6 Effective medium theory for corrected percolation threshold

The 2D Bruggeman effective medium theory predicts that the contact area percolates for $A/A_0=0.5$ independent of γ . However, numerical contact mechanics calculations for randomly rough surfaces predict that the contact area percolate for $A/A_0\approx 0.42$ for $\gamma=1$, and for $A/A_0>0.42$ when $\gamma<1$ and $A/A_0<0.42$ when $\gamma>1$. However, more studies are needed to determine the influence of finite-size effects, and to determine the $A_{\rm p}(\gamma)/A_0$ curve for large systems.

In ref. [27] it was suggested how to modify the Bruggeman effective medium theory so that it correctly reproduces the percolation for $A_{\rm p}/A_0\approx 0.42$. The resulting theory was found to be in good agreement with exact numerical results for the flow conductivity. Here we will show how to generalize this treatment to the case of anisotropic roughness.

Following ref. [27] we first consider a system in n dimension (in the study above, n=2). In this case (31) and (32) are generalized to

$$\frac{1}{\sigma_x} = \left\langle \frac{(n-1) + \gamma^*}{\sigma + \gamma^* (n-1)\sigma_x} \right\rangle,$$

$$\frac{1}{\sigma_y} = \left\langle \frac{(n-1) + (1/\gamma^*)}{\sigma + (1/\gamma^*)(n-1)\sigma_y} \right\rangle.$$

Following the approach in sect. 4 we get at percolation:

$$1 = \frac{(n-1) + \gamma^*}{\gamma^*(n-1)} \frac{A_p}{A_0},$$

$$1 = \frac{(n-1) + 1/\gamma^*}{(1/\gamma^*)(n-1)} \frac{A_p}{A_0},$$

which gives $\gamma^* = 1$ and

$$\frac{A_{\mathbf{p}}}{A_0} = \frac{n-1}{n} \,.$$

Thus, given A_p/A_0 obtained from (exact) numerical simulations, if we choose

$$n = \frac{1}{1 - A_{\rm p}/A_0}$$

then the (modified) effective medium theory will result in a flow conductivity which vanishes when the (normalized) contact area reaches the value $A_{\rm p}/A_0$ where the contact area percolate.

7 The critical junction theory of fluid flow

Consider a rubber seal. Assume first isotropic roughness and that the nominal contact region between the rubber and the hard counter-surface is a square area $L \times L$. We assume that a high-pressure fluid region occurs for x < 0and a low-pressure region for x > L. Now, let us study the contact between the two solids as we increase the magnification ζ . We define $\zeta = L/\lambda$, where λ is the resolution. We study how the apparent contact area (projected on the xyplane), $A(\zeta)$, between the two solids depends on the magnification ζ . At the lowest magnification we cannot observe any surface roughness, and the contact between the solids appears to be complete i.e., $A(1) = A_0$. As we increase the magnification we will observe some interfacial roughness, and the (apparent) contact area will decrease. At high enough magnification, say $\zeta = \zeta_c$, a percolating path of non-contact area will be observed for the first time. We denote the most narrow constriction along this percolation path as the critical constriction. The critical constriction will have the lateral size $\lambda_{\rm c} = L/\zeta_{\rm c}$ and the surface separation at this point is denoted by u_c . We can calculate u_c using a recently developed contact mechanics theory [2]. As we continue to increase the magnification we will find more percolating channels between the surfaces, but these will have more narrow constrictions than the first channel which appears at $\zeta = \zeta_c$, and as a first approximation one may neglect the contribution to the leak rate from these channels. An accurate estimate of the leak rate is obtained by assuming that all the leakage occurs through the critical percolation channel, and that the whole pressure drop $\Delta P = P_{\rm a} - P_{\rm b}$ (where $P_{\rm a}$ and $P_{\rm b}$ is the pressure to the left and right of the seal) occurs over the critical constriction (of width and length $\lambda_c \approx L/\zeta_c$ and height $u_{\rm c}$). We refer to this theory as the critical-junction theory. If we approximate the critical constriction as a pore with rectangular cross-section (width and length λ_c and height $u_{\rm c} \ll \lambda_{\rm c}$), and if we assume an incompressible Newtonian fluid, the volume flow per unit time through the critical constriction will be given by (Poiseuille flow)

$$\dot{Q} = \frac{u_{\rm c}^3}{12\eta} \Delta P. \tag{37}$$

In deriving (37) we have assumed laminar flow and that $u_c \ll \lambda_c$, which is always satisfied in practice. The flow conductivity σ_{eff} can be obtained from \dot{Q} using $\dot{Q} = J_x L = \sigma_{\text{eff}}(\Delta P/L)L$ giving

$$\sigma_{\text{eff}} = \frac{u_{\text{c}}^3}{12\eta} \,. \tag{38}$$

The following qualitative picture underpins the critical constriction model. At the critical magnification several fluid conducting channels may appear and each of them may have several critical constrictions as indicated in fig. 5(a). Now when we perform the mapping indicated in fig. 2, where we go from isotropic roughness in a square area $L \times L$ to the anisotropic roughness in a square area of the same size (dashed square in fig. 2(c)), we increase the number of flow channels in the x-direction by a factor of $\gamma^{1/2}$, and on each flow channel we reduce the number of critical junctions by a factor of $\gamma^{-1/2}$. Hence the fluid conductivity $\sigma_x = \gamma \sigma_0$. In a similar way one can show

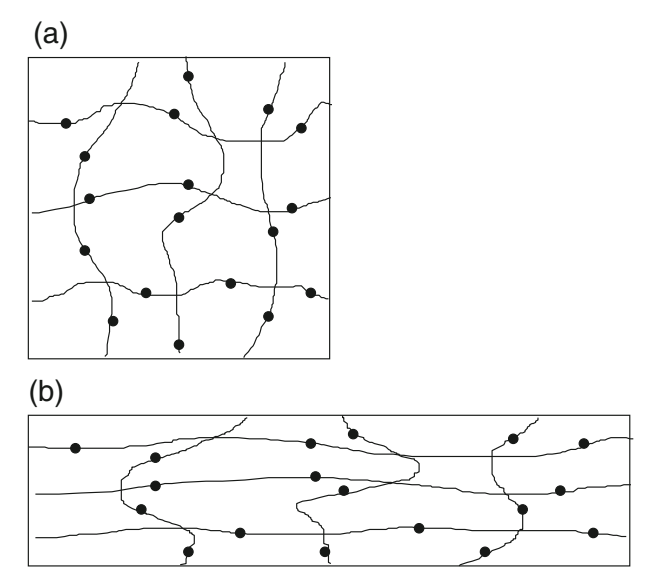


Fig. 5. (a) Percolating fluid flow channels (lines) and critical constrictions (black dots) for a $L \times L$ square unit system with isotropic roughness. (b) The percolating fluid flow channels and critical constrictions for a system obtained by stretching by a factor of 2 in the x-direction and 1/2 in the y-direction (Pekeling number $\gamma = 4$). After this mapping, the concentration of flow channels is increased by a factor of 2 in the x-direction and reduced by a factor of 1/2 in the y-direction. For a square unit $L \times L$ (not shown) the number of critical constrictions along each percolating flow channel is reduced by a factor of 1/2 in the x-direction and increased by a factor of 2 in the y-direction. The net result is that the fluid flow conductivity is increased by a factor of 4 in the x-direction and reduced by a factor of 1/4 in the y-direction, i.e., $\sigma_x = \gamma \sigma_0$ and $\sigma_y = \sigma_0/\gamma$, where σ_0 is the flow conductivity for the system with isotropic roughness in (a).

that $\sigma_y = \sigma_0/\gamma$. Note that this implies $\sigma_x = \gamma^2 \sigma_y$, which we derived above from the effective medium theory close to the contact area percolation threshold. Note that this agreement with the effective medium theory requires that the fluid pressure drop over a critical constriction is not modified by the stretching-contraction of the system.

To illustrate the accuracy of the critical junction approach, in fig. 6 I show the fluid pressure flow factor $\phi_{\rm p}=12\eta\sigma_x/\bar{u}^3$ as a function of the average surface separation \bar{u} (log-log scale). In the calculation we have used the surface roughness power spectra shown in fig. 7 and Young's elastic modulus $E=10\,\mathrm{MPa}$. Results are shown for $\gamma = 1$ (red curves) and $\gamma = 4$ (blue curves) using the effective medium theory (solid lines) and the critical junction theory (dashed curves). In all the calculation we have assumed $A_{\rm p}/A_0 = 0.42$ independent of γ . As expected, the critical junction theory is accurate when the average surface separation is small enough but is inaccurate for very small contact pressures where the average surface separation is large; this is expected as for large average surface separation a nearly uniformly thick fluid film separate the surfaces and the fluid pressure drop will not occur over a small number of narrow constrictions, but will occur nearly uniformly over the whole nominal

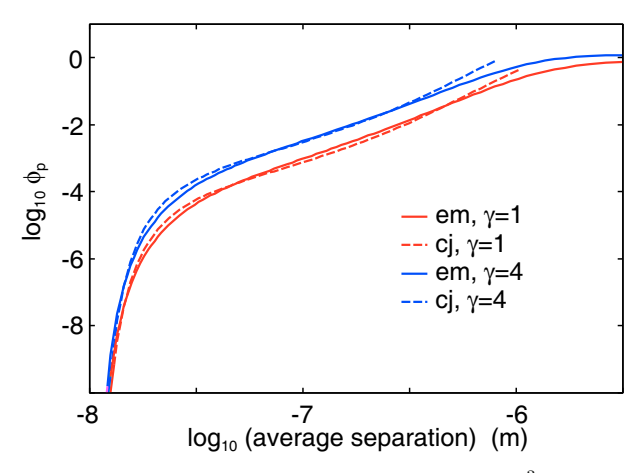


Fig. 6. Fluid pressure flow factor $\phi_{\rm p}=12\eta\sigma_x/\bar{u}^3$ as a function of the average surface separation \bar{u} (log-log scale). In the calculation we have used the surface roughness power spectra shown in fig. 7 and Young's elastic modulus $E=10\,{\rm MPa}$. Results are shown for $\gamma=1$ (red curves) and $\gamma=4$ (blue curves) using the effective medium (em) theory (solid lines) and the critical junction (cj) theory (dashed curves).

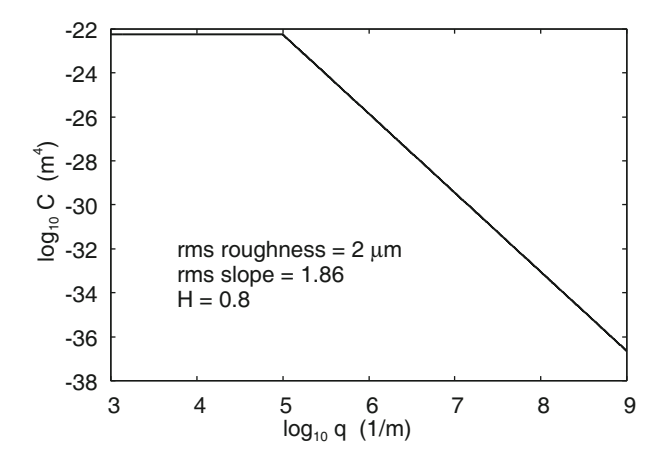


Fig. 7. Surface roughness power spectrum as a function of the wavenumber (log-log scale).

contact area. However, this limiting case is not of interest in sealing applications.

8 Discussion

In ref. [22] we used molecular dynamic simulations to study the percolation of the contact area with increasing pressure for Tripp numbers $0.5 < \gamma < 2$. We found that the results could be reasonably well fit with the formula $A_{\rm p}/A_0 = \gamma/(1+\gamma)$. However, the Bruggeman effective medium theory predicts $A_{\rm p}/A_0 = 0.5$ independent of γ . The effective medium theory for anisotropic roughness is based on stretching the contact area obtained for isotropic roughness. In this case it is clear from very simple arguments (see sect. 2) that for an infinite system the percolation threshold does not depend on the asymmetry (or stretching) parameter γ . However, the numerical studies are for surfaces with stretched surface roughness profiles.

In this case the simulations indicate that $A_{\rm p}/A_0$ depends on γ . This may be a finite-size effect, but a recent study indicates that A/A_0 at the percolation threshold may depend on γ also for infinite system size.

Recently, Yang et al. have performed a numerical study of the effect of surface roughness anisotropy on the percolation threshold of sealing surfaces [15]. For surfaces with isotropic roughness they found $A_{\rm p}/A_0\approx 0.48$, i.e., close to the effective medium theory prediction, and larger than the value 0.42 found by Dapp et al. [27]. As γ increased from 0.5 to 1.66, Yang et al. found that A/A_0 increased from 0.43 to 0.53, which is a weaker γ -dependence than given by $A_{\rm p}/A_0=\gamma/(1+\gamma)$, which predicts that $A_{\rm p}/A_0$ increases from 0.33 to 0.63.

The good agreement found between the effective medium theory and the critical junction theory indicates that the basic picture behind the critical junction theory is accurate. The critical junction theory is based on the observation that when increasing the magnification, at high enough magnification, say $\zeta = \zeta_c$, a percolating path of non-contact area will be observed for the first time. As we continue to increase the magnification we find more percolating channels between the surfaces, but these will have more narrow constrictions than the first channel which appears at $\zeta = \zeta_c$, and as a first approximation one may neglect the contribution to the leak rate from these channels. This implies that the roughness observed when the magnification is increased beyond $\zeta = \zeta_c$ has a negligible influence on the leakage of a seal. I a recent comment, Papangelo et al. [16] state that the leakage rate depends on the short distance cut-off length λ_1 (observed at the highest magnification ζ_1), which could be an atomic distance, but this is in general not the case unless then nominal pressure is so high as to move the critical constriction to the shortest length scale, which is nearly never the case in practical applications.

9 Summary and conclusion

I have shown that the Bruggeman effective medium theory and the critical junction theory give nearly the same results for the fluid flow conductivity (and the fluid pressure flow factor). This shows (qualitatively) that, unless the nominal contact pressure is so high at to result in nearly complete contact, the surface roughness observed at high magnification is irrelevant for the fluid flow during squeeze-out, or for the leakage of stationary seals.

The effective medium theory predicts that the fluid flow conductivity vanishes at the relative contact area $A/A_0=0.5$ independent of the anisotropy. However, the effective medium theory does not solve the elastic contact mechanics problem but is based on a purely geometric argument. Thus, for anisotropic roughness the contact area may percolate at different values of A/A_0 depending on the direction. I have discussed how this may be taken into account in the effective medium and critical junction theories.

The flow conductivity studied in this paper determines the pressure flow factor which enters in the (by the surface roughness) modified Reynolds equation of fluid flow between closely spaced solids in relative motion. The second (shear) flow factor which enters in this theory can be calculated using the equations derived in ref. [4]. The complete theory predicts the influence of surface roughness on problems like the transition from hydrodynamic to boundary lubrication (the Stribeck curve), or the friction and fluid leakage in dynamic seals.

Open Access Funding provided by Projekt DEAL. I thank M. Scaraggi for useful comments on the manuscript and M. Müser for critical discussions related to the influence of surface anisotropy on the contact area percolation problem.

Publisher's Note The EPJ Publishers remain neutral with regard to jurisdictional claims in published maps and institutional affiliations.

Appendix A. Two integrals

In sects. 3 and 4 appeared two important integrals

$$I_1 = \frac{1}{2\pi} \int_0^{2\pi} d\phi \frac{\cos^2 \phi}{\cos^2 \phi + \gamma^2 \sin^2 \phi} = \frac{1}{1+\gamma},$$
 (A.1)

$$I_2 = \frac{1}{2\pi} \int_0^{2\pi} d\phi \, \frac{\sin^2 \phi}{\cos^2 \phi + \gamma^2 \sin^2 \phi} = \frac{1}{\gamma (1+\gamma)} \,. \quad (A.2)$$

Note that $I_1 + \gamma^2 I_2 = 1$. The results above can the proved by integration in the complex plane: Introducing $z = e^{i\phi}$ and writing $\cos \phi = (z+1/z)/2$ and $\sin \phi = (z-1/z)/(2i)$ and performing the integration around the circle |z|=1 results in eqs. (A.1) and (A.2).

Appendix B. Flow current in elliptic insertion

The 2D fluid flow problem is mathematically similar to the electrostatic polarization of a dielectric material. Thus the fluid flow current and the electric current both satisfy $\nabla \cdot \mathbf{J} = 0$ (conservation of fluid volume and electric charge, respectively). The fluid current is related to the pressure gradient via $\mathbf{J} = -\sigma \nabla p$, where σ is the flow conductivity, and the electric current is related to the electric potential via $\mathbf{J} = -\sigma \nabla \phi$, where σ is the electric conductivity. Hence, results obtained in electrostatics for polarizable media can be used also for the fluid flow problem. In particular, from electrostatics it is known that if an elliptic region with constant dielectric properties is embedded in an infinite dielectric material with other dielectric properties, then the electric field (and hence the polarization) in the elliptic region will be constant, assuming that the electric field is constant far away from the elliptic region. The corresponding result for the fluid flow problem was used in sect. 4.

Note that when σ is constant the equation $\nabla \cdot \mathbf{J} = 0$ gives $\nabla^2 p = 0$ (for fluid flow) and $\nabla^2 \phi = 0$ (for electrostatics). The results for the electric polarization problem for

an elliptic insertion can be derived by solving the Laplace equation $\nabla^2 \phi = 0$ using elliptic coordinates [28] or by complex mapping methods [29].

Open Access This is an open access article distributed under the terms of the Creative Commons Attribution License (http://creativecommons.org/licenses/by/4.0), which permits unrestricted use, distribution, and reproduction in any medium, provided the original work is properly cited.

References

- C. Rotella, B.N.J. Persson, M. Scaraggi, P. Mangiagalli, Eur. Phys. J. E 43, 9 (2020).
- C. Yang, B.N.J. Persson, J. Phys.: Condens. Matter 20, 215214 (2008).
- 3. Martin H. Müser, Wolf B. Dapp, Romain Bugnicourt, Philippe Sainsot, Nicolas Lesaffre, Ton A. Lubrecht, Bo N.J. Persson, Kathryn Harris, Alexander Bennett, Kyle Schulze, Sean Rohde, Peter Ifju, W. Gregory Sawyer, Thomas Angelini, Hossein Ashtari Esfahani, Mahmoud Kadkhodaei, Saleh Akbarzadeh, Jiunn-Jong Wu, Georg Vorlaufer, András Vernes, Soheil Solhjoo, Antonis I. Vakis, Robert L. Jackson, Yang Xu, Jeffrey Streator, Amir Rostami, Daniele Dini, Simon Medina, Giuseppe Carbone, Francesco Bottiglione, Luciano Afferrante, Joseph Monti, Lars Pastewka, Mark O. Robbins, James A. Greenwood, Tribol. Lett. 65, 118 (2017).
- B.N.J. Persson, M. Scaraggi, Eur. Phys. J. E 34, 113 (2011).
- Patir Nadir, Effect of Surface Roughness on Partial Film Lubrication Using an Average Flow Model Based on Numerical Simulation (University Microfilms, 1989).
- 6. N. Patir, H.S. Cheng, J. Lubr. Technol. 100, 12 (1978).
- 7. N. Patir, H.S. Cheng, J. Lubr. Technol. 101, 220 (1979).
- F. Sahlin, A. Almqvist, R. Larsson, S.B. Glavatskih, Tribol. Int. 40, 1025 (2007).
- 9. J.H. Tripp, J. Lubr. Technol. 105, 458 (1983).
- A. Almqvist, J. Fabricius, A. Spencer, P. Wall, J. Tribol. 133, 031702 (2011).
- B.N.J. Persson, C. Yang, J. Phys.: Condens. Matter 20, 315011 (2008).
- 12. B. Lorenz, B.N.J. Persson, Eur. Phys. J. E 31, 159 (2010).
- 13. B. Lorenz, B.N.J. Persson, Eur. Phys. J. E 32, 281 (2010).
- B.N.J. Persson, N. Prodanov, B.A. Krick, N. Rodriguez, N. Mulakaluri, W.G. Sawyer, P. Mangiagalli, Eur. Phys. J. E 35, 5 (2012).
- Z. Yang, J. Liu, X. Ding, F. Zhang, J. Tribol. 141, 022203 (2019).
- 16. A. Papangelo, M. Ciavarella, J. Tribol. 142, 065501 (2020).
- Z. Yang, J. Liu, X. Ding, F. Zhang, J. Tribol. 142, 066001 (2020).
- 18. A. Wang, M.H. Müser, Finite size effects of the contact area percolation threshold for systems with anisotropic roughness, in preparation.
- 19. J. Peklenik, Proc. Inst. Mech. Eng. 182, 108 (1967).
- 20. L. Afferrante, F. Bottiglione, C. Putignano, B.N.J. Persson, G. Carbone, Tribol. Lett. **66**, 75 (2018).
- A. Almqvist, C. Campana, N. Prodanov, B.N.J. Persson, J. Mech. Phys. Solids 59, 2355 (2011).

- B.N.J. Persson, J. Phys.: Condens. Matter 22, 265004 (2010).
- 23. D.A.G. Bruggeman, Ann. Phys. (Leipzig) 24, 636 (1935).
- 24. P.A. Fokker, Transp. Porous Media 44, 205 (2001).
- 25. M. Scaraggi, Phys. Rev. E 86, 026314 (2012).
- M. Scaraggi, Proc. R. Soc. A: Math. Phys. Eng. Sci. 471, 20140739 (2015).
- W.B. Dapp, A. Lücke, B.N.J. Persson, M.H. Müser, Phys. Rev. Lett. 108, 244301 (2012).
- 28. P.M. Morse, H. Feshbach, Methods of Theoretical Physics, Part 2 (McGraw Hill, 1953) p. 1199.
- 29. P.J. Olver, Complex Analysis and Conformal Mapping (University of Minnesota, 2018).